JACS
JOURNAL OF THE AMERICAN CHEMICAL SOCIETY
pubs.acs.org/JACS
Article

Outcompeting Thermodynamics: Ion-Pairing and Coulombic Interactions to Trigger Perfluoroacetate Intra-Ionic Photooxidation for Perfluoroalkylation Reactions

Pengju Li, Céline Bourgois, Felix Glaser, Simon De Kreijger, Alejandro Cadranel, Ludovic Troian-Gautier,* and Ke Hu*

Cite This: J. Am. Chem. Soc. 2025, 147, 12082−12091
Read Online
ACCESS | Metrics & More | Article Recommendations | Supporting Information

ABSTRACT: Trifluoromethylation is a key transformation in drug and agrochemical synthesis, yet current reagents often suffer from high cost, low atom economy, and low scalability. Trifluoroacetate derivatives represent ideal reagents as they are highly abundant and cheap, but their very positive one electron oxidation potential (~2.3 V vs NHE) often hampers their widespread use in photoredox catalysis. Indeed, at these potentials, selectively oxidizing trifluoroacetate over reaction solvent or partner substrates becomes challenging. Herein, we present a novel approach that circumvents these limitations through the use of a pentacationic Ir(III) photosensitizer that forms a strong 1:1 ion-pair with trifluoroacetate in acetonitrile (K_{eq} = 6 × 10^4 M^{-1}). This ion-pair formation enables rapid and efficient photooxidation of trifluoroacetate in ~90 ps without significant solvent or partner substrate oxidation, as indicated by femtosecond and nanosecond UV−visible transient absorption spectroscopy. The $CF_3^•$ radicals so generated are shown to trifluoromethylate a range of partner substrates, including aromatic compounds, heterocycles, natural products and pharmaceutically relevant products, in moderate yields (20−60%). Control experiments reveal that ion-pairing is crucial for the successful generation of $CF_3^•$ as photosensitizers that oxidize trifluoroacetate without forming ion pairs were ineffective for trifluoromethylation. This probably originates from the more thermodynamically accessible substrate oxidation outcompeting diffusional trifluoroacetate oxidation. The reaction was further exemplified to allow functionalization with a variety of perfluoroalkyl groups of different chain lengths. The approach reported herein could also be used for the removal and/or use of perfluoroalkyl substances (PFAS), often called "forever chemicals", that have recently raised environmental and health concern.

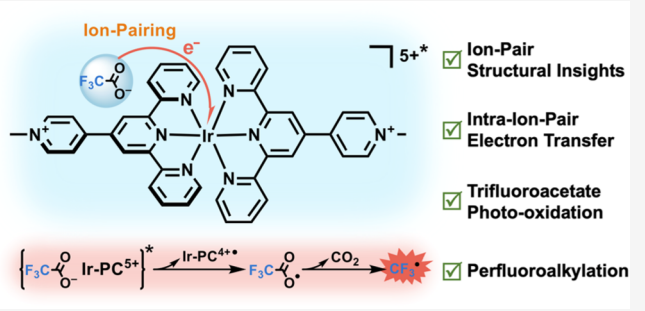

INTRODUCTION

Photoredox catalysis has revolutionized the synthetic organic chemistry landscape by providing novel means to perform challenging transformations.[1−8] Among them, selective trifluoromethylation of C−H bonds represents an important class of reactions as over 20% of pharmaceutical drugs and 30% of agrochemical compounds contain fluorine atoms.[9−11] Previous synthetic methods that utilize nucleophilic or electrophilic trifluoromethylating reagents have thus far spearheaded advances for these applications.[12−17] Some of the most useful precursors for this chemistry include the famous Togni's reagents based on hypervalent iodine derivatives[18] or Teruo,[19,20] Shreeve[21] and Shibata's[22] reagents based on sulfonium or selenophenium derivatives, among others (Figure 1). Despite these advances, these reagents suffer from poor atom economy and high costs that hampers large scale implementation. Hence, alternative approaches for the trifluoromethylation of organic substrates are clearly needed.

Trifluoroacetate derivatives represent ideal candidates as CF_3 sources due to their high abundance, low cost and good atom economy. Indeed, the only byproduct of $CF_3^•$ generation from trifluoroacetate oxidation is gaseous CO_2 that facilitates separation and purification. The use of trifluoroacetate has previously been reported from which a key challenge was identified. The very unfavorable one electron oxidation occurs at potential near ~2.3 V vs NHE where competitive oxidation of other substrates and solvent occurs (Figure 1).[24−31] Also, auxiliaries to tune the redox potential were investigated in the past, but they often rely on stoichiometric auxiliary reagents for trifluoroacetate activation.[23] Thus, existing electrochemical and photochemical approaches for the trifluoromethylation of

Received: January 4, 2025
Revised: March 3, 2025
Accepted: March 21, 2025
Published: March 31, 2025

https://doi.org/10.1021/jacs.5c00129
J. Am. Chem. Soc. 2025, 147, 12082−12091

organic substrates with trifluoroacetate reagents are limited to specific solvents and reaction conditions.

Heterogeneous materials have been investigated for trifluoromethylation of organic substrates. In 1993, Mallouk and co-workers were among the first to report the photochemical generation of $CF_3^\bullet$ from silver trifluoroacetate using TiO_2 as photocatalyst and a Hg lamp.[24] This photo-Kolbe decarbonylation reaction occurred efficiently in acetonitrile as the trifluoroacetate was adsorbed to the TiO_2 via the carboxylate functional group. Several substrates were trifluoromethylated with yields that ranged from 10 to 50%. Other heterogeneous photoactive materials have recently been reported using a similar approach. For example, Li and co-workers used Rh-modified TiO_2 nanoparticles in combination to trifluoroacetic acid to generate trifluoromethylated derivatives in moderate to good yields concomitantly to hydrogen production.[33] Hosseini-Sarvari and co-workers used Au@ZnO core−shell materials in combination to trifluoroacetate and 400−495 nm irradiation to generate trifluoromethylated products in moderate to good yields.[34] Very recently, a heterogeneous photoelectrocatalytic system composed of a molybdenum-doped tungsten trioxide (WO_3) photoanode and trifluoroacetate derivatives was used for large scale (100 g) trifluoromethylation reactions in moderate yields using an applied potential of 2 V and 390 nm irradiation.[26]

These heterogeneous systems are proposed to operate by association of the trifluoroacetate with the oxide surface. Photon absorption then triggers prompt and efficient interfacial oxidation through an inner-sphere type mechanism with generation of the corresponding $CF_3^\bullet$. It is therefore unsurprising that photoredox chemists have also used these inner-sphere oxidation mechanisms to develop robust alternatives to produce $CF_3^\bullet$. Such inner-sphere oxidation is often reported to occur via ligand-to-metal charge transfer (LMCT) excitation between a trifluoroacetate derivative and a high-valent metal center within the 3d block such as Fe(III), Cu(II), or Ti(IV). Upon excitation, a ligand-based filled orbital donates an electron to an empty or partially filled metal-centered orbital, thus decreasing the M−L bond order, often leading to the formation of a reduced metal complex and a radical product.[37,38] Notable examples include the reports of the groups of West,[25] Li,[39] Niu[36] and Juliá-Hernández[35] that all used LMCT excitation of Fe-trifluoroacetate derivatives using UV or blue light irradiation in combination to some additives to generate the desired trifluoromethylated products with yields of up to 87%. Nocera and co-workers recently reported the electrophotocatalytic perfluoroalkylation reaction through LMCT excitation of Ag(II) perfluoroalkyl carboxylate derivatives coupled to electrochemistry.[30] These LMCT activations are highly attractive as they operate using abundant sources such as trifluoroacetate and iron salts, in combination to other additives that are not described herein. Due to the mixture of different additives and reversible ligand coordination, these systems often have limited understanding of the reactive structure and pathway as these photoactive species are usually formed *in situ*. Outer-sphere oxidation have also been reported using Ru(II) and Ir(III) photosensitizers[40] but they often rely on the use of activated forms of trifluoroacetates[23,29] or the need for additives that complexify the mechanistic analysis.[28]

Herein, we report an approach that uses a well-defined pentacationic Ir(III) photosensitizer[41] that is shown to form a 1:1 ion-pair with trifluoroacetate in acetonitrile. Steady-state and time-resolved spectroscopic techniques were used to investigate the ion-pair reactivity upon visible light irradiation. Stern−Volmer experiments confirmed that the excited-state quenching occurred from the preassociated trifluoroacetate. Mechanistic study revealed that the quenching process operated via electron transfer from the trifluoroacetate to the excited iridium photosensitizer that generated the reduced iridium photosensitizer and the corresponding $CF_3^\bullet$ with a cage escape yield of 0.056. This photogenerated $CF_3^\bullet$ was further used for trifluoromethylation of organic substrates in moderate yields. The results are compared with prototypical photosensitizers that share the ability to photo-oxidize trifluoroacetate but do not form ion-pairs. In these cases, trifluoromethylation was not operative. This indicated the synergistic effects of ion-pairing between trifluoroacetates and the pentacationic Ir(III) photosensitizers to trigger trifluoroacetate oxidation (and thus lead to perfluorination) over the oxidation of partner substrate present in the reaction medium. The reaction scope was then extended to a series of natural products and pharmaceuticals and further expanded to allow functionalization with C_2F_5, C_3F_7, C_4F_9, C_5F_{11}, and C_6F_{13} groups.

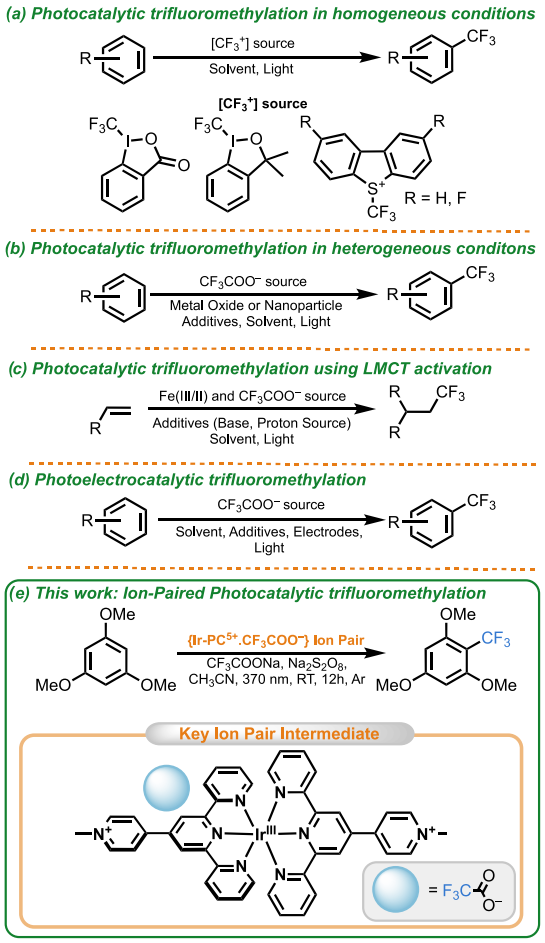

Figure 1. Selected examples of photocatalytic trifluoromethylation reactions operating (a) in homogeneous conditions,[32] (b) in heterogeneous conditions,[24,33,34] (c) via ligand-to-metal charge transfer (LMCT) activation,[25,35,36] (d) via photoelectrocatalysis,[26,27,30] and (e) via ion-pair formation (this work). See introduction for additional details.

https://doi.org/10.1021/jacs.5c00129
J. Am. Chem. Soc. 2025, 147, 12082−12091

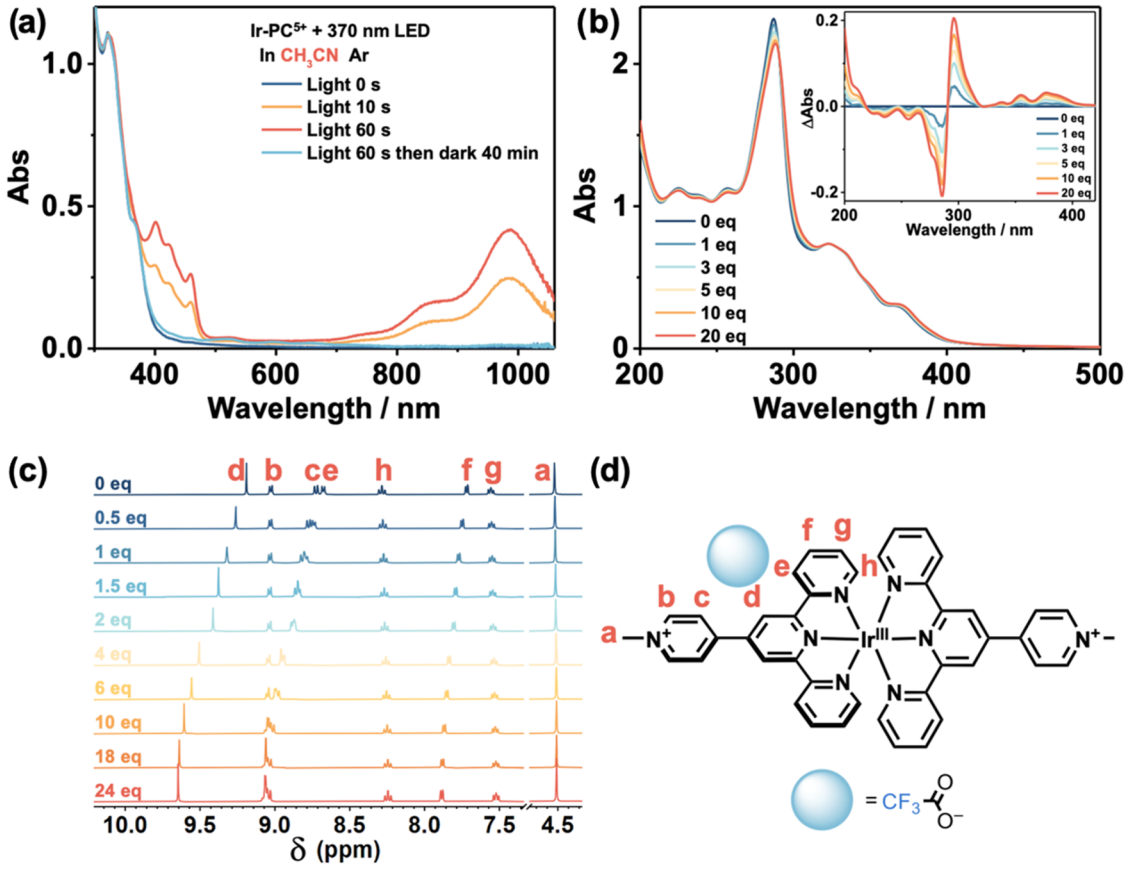

Figure 2. (a) Absorption changes of **Ir-PC**$^{5+}$ under 370 nm LED light irradiation (400 mW/cm^2) at indicated times in argon-purged CH_3CN. (b) Absorption changes of 20 μM **Ir-PC**$^{5+}$ upon titration of CF_3COONa from 0 to 20 equiv in CH_3CN. The inset shows the difference between the absorption spectrum after each addition of CF_3COONa and the initial spectrum. (c) ^{1}H NMR spectra of 1 mM **Ir-PC**$^{5+}$ at indicated equivalents of CF_3COONa in CD_3CN. (d) Structure and H atoms labels for **Ir-PC**$^{5+}$.

RESULTS AND DISCUSSION

$[Ir(tpy\text{-}PyMe)_2]^{5+}$ (**Ir-PC**$^{5+}$) is an Ir(III) photosensitizer bearing two 2,2′:6′,2″-terpyridine ligands decorated by *N*-methylpyridinium units, thereby formally generating a pentacationic species (Figure 1e).[41] This photosensitizer absorbs light intensely at 360 nm that tails up to 450 nm. Excitation of this photosensitizer leads to well-resolved photoluminescence that is in line with a predominant ligand-centered (^{3}LC) excited state. The photoluminescence decay was well resolved with a single exponential that led to an excited-state lifetime of 3.77 μs in acetonitrile under argon. From the photoluminescence, an E_{0-0} value of 2.63 eV was determined which allowed, with the ground-state reduction potential of −0.23 V vs NHE, to estimate the corresponding excited-state reduction potential, E_{red}* = 2.40 V vs NHE.

It is noteworthy that this value matches the required potential to oxidize sodium trifluoroacetate (~2.3 V vs NHE) but, as previously alluded to in the introduction, such a value is so positive that it would impose restrictions in terms of solvent and substrate scope. In here, rather than investigating a limited subset of substrates and solvents with wide electrochemical windows or using solvents that are not sustainable on an economic or ecological standpoint, we used acetonitrile, *i.e.* a solvent that is suitable for photoredox catalysis and spectroscopic measurements. We hypothesized that forming ion-pairs between reactive species would improve and accelerate the reaction of the ion-paired species,[42,43] favoring trifluoroacetate oxidation over acetonitrile and/or substrate oxidation. To test this hypothesis, we first investigated the excited-state reactivity of **Ir-PC**$^{5+}$ in acetonitrile. LED light irradiation at 370 nm led to the full formation of the monoreduced **Ir-PC**$^{4+\bullet}$ in 60 s, as indicated by the novel absorption features observed around 400 nm and between 800 and 1000 nm (Figure 2a). These novel features are in line with spectroelectrochemical experiments.[41] Thus, 370 nm light irradiation leads to the formation of the monoreduced **Ir-PC**$^{4+\bullet}$ photosensitizer, presumably through the oxidation of acetonitrile, and this reaction is reversible as the initial authentic spectrum of **Ir-PC**$^{5+}$ is recovered after 40 min in the dark.

We then focused on investigating the ground-state interaction between trifluoroacetate and **Ir-PC**$^{5+}$. The UV−visible absorption spectrum of **Ir-PC**$^{5+}$ was monitored upon the increased addition of sodium trifluoroacetate from 0 to 20 equiv (Figure 2b). The addition of sodium trifluoroacetate led to significant UV−visible absorption changes, with a notable decrease at 285 nm and a corresponding increase at 295 nm. These changes are further visualized in the difference spectra (Figure 2b, Inset) and are in line with the formation of an ion-pair between **Ir-PC**$^{5+}$ and trifluoroacetate. A binding constant of 1.3×10^4 M^{-1} was determined from a Benesi−Hildebrand type analysis of the UV−visible titration (Figure S1).[44] The stoichiometry of that ion-pair was investigated through a job plot analysis of the UV−visible data that revealed that it occurred in a 1:1 fashion (Figure S2). At this stage, it is complicated to understand why only one trifluoroacetate

https://doi.org/10.1021/jacs.5c00129
J. Am. Chem. Soc. 2025, 147, 12082−12091

would bind this pentacationic photosensitizer. It is plausible that the other PF_6^- counterions are also exchanged by CF_3COO^- but do not lead to significant changes in the UV−visible absorption spectra.

The position of the ion-paired trifluoroacetate was then investigated using the atomic resolution provided by ^{1}H NMR. The addition of sodium trifluoroacetate to a 1 mM solution of **Ir-PC^{5+}** in deuterated acetonitrile led to the change in chemical shift of certain proton resonances (Figures 2c,d, S3−S4). Interestingly, the peak at 4.52 ppm, attributed to the methyl of the *N*-methyl-pyridinium fragment, was unaffected by the addition of up to 24 equiv of sodium trifluoroacetate. This indicated that, despite the localized positive charge, this moiety is not involved in the ion-paired process. The chemical shifts that were the most influenced by the addition of trifluoroacetate correspond to those of protons *c* (8.73 ppm), *d* (9.19 ppm), and *e* (8.67 ppm) (Figure 2c). Indeed, proton *c* exhibited a shift from 8.73 to 9.06 ppm while proton *e* and *d* exhibited shifts from 8.67 to 9.03 ppm and from 9.19 to 9.65 ppm, respectively. These large shifts are in line with the interaction of trifluoroacetate with that portion of the terpyridine backbone (Figure 2d). A plot of the change in chemical shift (Δppm) as a function of the concentration of trifluoroacetate allowed to extrapolate a binding constant of 5.4 × 10^2 M^{-1} (Figure S4). This value is smaller than the one determined by UV−visible absorption, as reported for other systems in the literature.[45] Additional titration experiments using the ligand only did not show significant shifts by UV−visible absorption spectroscopy or by ^{1}H NMR (Figure S5 and S6). Thus, the efficient binding of trifluoroacetate to the **Ir-PC^{5+}** is most likely related to the overall charge of the photosensitizer that offers a favorable environment for the binding event (Figure 2d).

The excited-state reactivity of **Ir-PC^{5+}** with sodium trifluoroacetate was then investigated in acetonitrile through classical Stern−Volmer experiments. The time-resolved photoluminescence spectra of **Ir-PC^{5+}** was recorded with increasing amounts of sodium trifluoroacetate, which led not only to a drastic decrease of the excited-state lifetime but also of the initial amplitude (α) (Figure 3a). Stern−Volmer analysis was performed using the excited-state lifetime (τ) which yielded the corresponding bimolecular quenching rate constant, $k_q = K_D/\tau_0 = 1.5 \times 10^{11}$ M^{-1} s^{-1}, where K_D is the diffusive quenching constant abstracted from the slope of the linear fit and τ_0 is the excited-state lifetime in the absence of quencher (shown in Figure 3b, inset, and eqs S4−5). At first glance, this value appears larger than the diffusion limit in acetonitrile but it is actually in line when the respective charges of the photosensitizer and quencher are taken into consideration.[46−49] Indeed, the pentacationic Ir(III) photosensitizer and the trifluoroacetate exhibit Coulombic attraction which increases the diffusion limit. Similar effects have also been observed for polycationic Ru(II) photosensitizers used for the photooxidation of halides.[50,51]

A plot of the initial amplitude in the absence of quencher (α_0) over the amplitude at each free concentration of sodium trifluoroacetate led to the determination of the equilibrium constant, $K_{eq} = 6.1 \times 10^4$ M^{-1} (Figure 3a inset). The Stern−Volmer plot for the uncorrected total concentration of sodium trifluoroacetate is shown in Figure S7. This equilibrium constant is on the same order of magnitude as the values determined by UV−visible absorption titration experiments. The slightly more positive value determined here could reflect

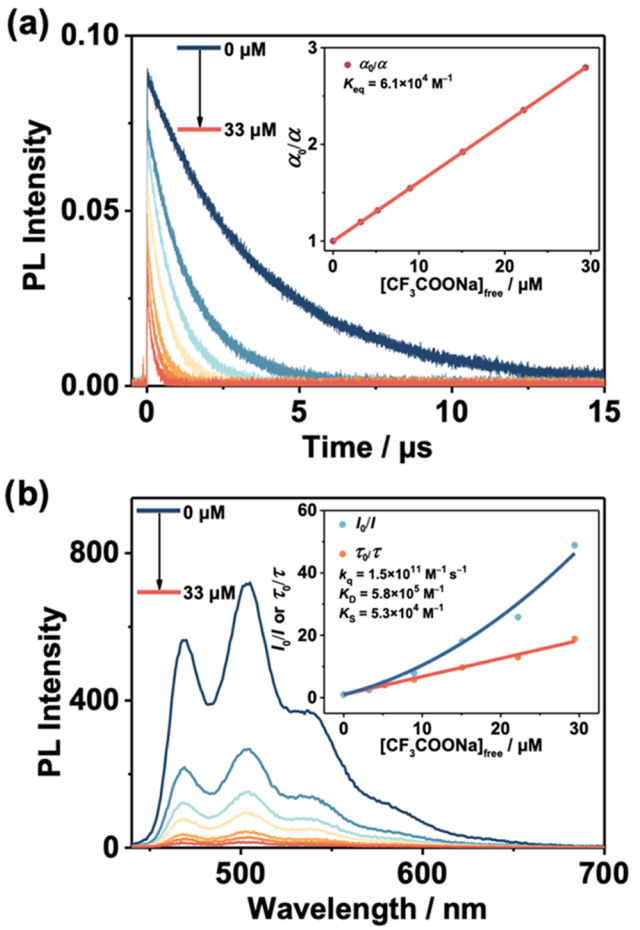

Figure 3. (a) Time-resolved photoluminescence quenching of **Ir-PC^{5+}** upon titration of CF_3COONa monitored at 505 nm in argon-purged CH_3CN after pulsed 355 nm laser excitation. The inset shows the initial amplitude quenching data for **Ir-PC^{5+}** plotted vs. $[CF_3COONa]_{free}$. (b) Steady-state photoluminescence spectra of **Ir-PC^{5+}** (λ_{ex} = 365 nm) upon titration of CF_3COONa in argon-purged CH_3CN. The inset shows the corresponding Stern−Volmer plots of the I_0/I *vs.* $[CF_3COONa]_{free}$ and τ_0/τ vs $[CF_3COONa]_{free}$ for the steady-state photoluminescence quenching and time-resolved photoluminescence quenching, respectively, monitored at 505 nm.

slight changes in binding upon excited-state formation. Interestingly, when the excited-state quenching experiments were performed using the steady-state photoluminescence intensity (I), the corresponding Stern−Volmer plots (Figure 3b, inset) exhibited upward quadratic curvature, indicative of the involvement of static quenching along with dynamic quenching (plot of τ_0/τ vs $[CF_3COONa]_{free}$ in Figure 3b, inset), in line with the preassociation of trifluoroacetate. The nonlinear Stern−Volmer plot could be accurately modeled using the predetermined K_D which allowed to yield the static quenching constant, $K_S = 5.3 \times 10^4$ M^{-1} (eq S6). This value is similar to the equilibrium constant previously determined from the initial time-resolved photoluminescence amplitude analysis. Thus, these Stern−Volmer experiments confirm that **Ir-PC^{5+}** is able to react with trifluoroacetate through a combination of static and dynamic quenching processes, presumably through excited-state electron transfer.

As these Stern−Volmer experiments do not indicate the nature of the quenching process, we turned to UV−visible nanosecond transient absorption spectroscopy. Pulsed light

https://doi.org/10.1021/jacs.5c00129
J. Am. Chem. Soc. 2025, 147, 12082−12091

excitation of **Ir-PC**$^{5+}$ in argon purged acetonitrile led to excited-state formation that exhibited enhanced excited-state absorption at wavelength between 400 and 700 nm (Figure 4). Upon the addition of trifluoroacetate, the transient absorption spectrum was severely modified, with notable absorption changes between 400 and 460 nm. These transient absorption changes matched well with the authentic spectra of the reduced iridium photosensitizer obtained by photolysis in the presence of triethylamine used as sacrificial electron donor (Figure S8). This confirmed that the quenching process occurred via electron transfer from trifluoroacetate to the excited **Ir-PC**$^{5+}$, thus generating the corresponding reduced photosensitizer and oxidized trifluoroacetate. Single wavelength absorption changes recorded in the presence and absence of trifluoroacetate confirmed efficient excited-state quenching and the formation of the reduced species that appeared through a combination of dynamic and static quenching and lived for several milliseconds (Figure S9). This long-lived charge separated species probably originates from the dissociation of the trifluoroacetate radical into the corresponding carbon dioxide and trifluoromethyl radical ($CF_3^{\bullet}$), thus changing the driving force and kinetics for back-electron transfer. The cage escape yield, i.e. the separation efficiency of both radicals formed after bimolecular electron transfer was also quantified using comparative actinometry methods and transient absorption spectroscopy.[52] Unfortunately, the determined cage escape yields are low, $\Phi_{CE} = 0.056$ (Figure S10), despite the scission of $CF_3COO^{\bullet}$ to form CO_2 and $CF_3^{\bullet}$ that would have potentially increased those yields. Thus, it appears that the scission of the $CF_3-COO^{\bullet}$ bond is slower than the geminate charge recombination. Similar results have been observed for the photoinduced scission of the $C-N_2^+$ bond of diazonium derivatives that occurs within 10 ns following pulsed light excitation.[53] Nevertheless, these experiments confirm efficient excited-state electron transfer but allow to postulate, given the small cage escape yields, that the subsequent trifluoromethylation could operate with moderate yields under standard irradiation times and conditions.

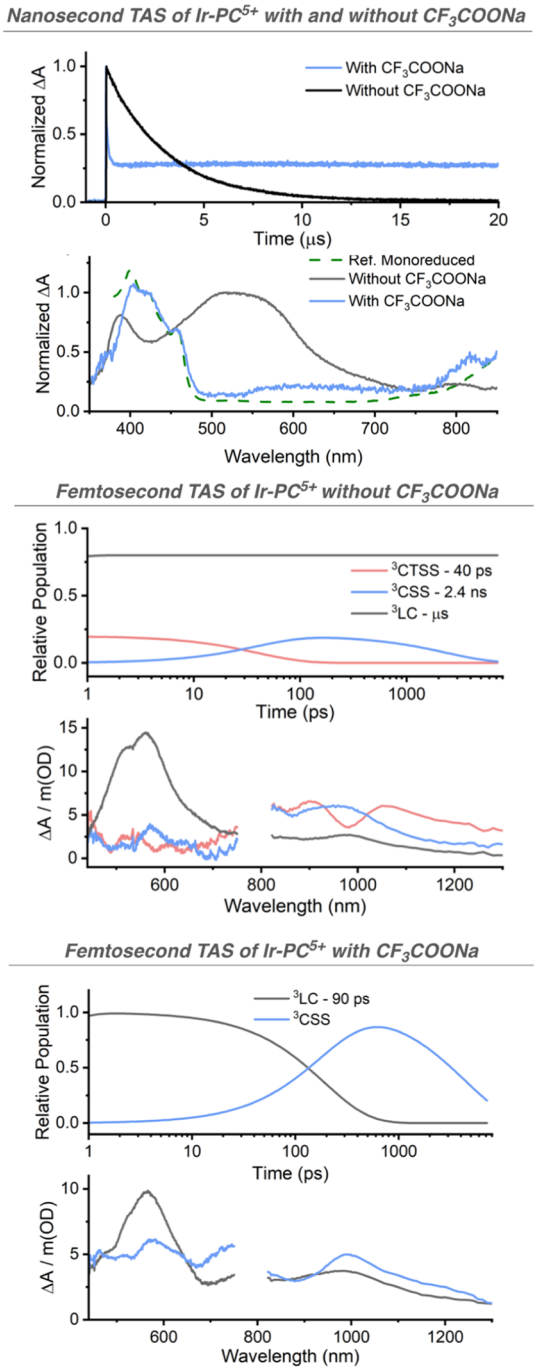

Figure 4. Nanosecond transient absorption difference spectra (top) of **Ir-PC**$^{5+}$ with (blue) and without (black) 2 mM CF_3COONa 500 ns after pulsed 355 nm laser excitation in argon-purged CH_3CN, along with the photolysis spectrum (dashed green) of **Ir-PC**$^{5+}$ using triethylamine (TEA) as the electron donor. The single wavelength absorption changes monitored at 550 nm for **Ir-PC**$^{5+}$ and at 457 nm for **Ir-PC**$^{5+}$ in the presence of CF_3COONa are also shown (top). Femtosecond transient absorption difference spectra recorded without (middle) and with (bottom) 2 mM CF_3COONa as well as the relative population based on global analysis. See text and Supporting Information for additional details.

With the aim of directly monitoring the intra-ion-pair electron transfer process, femtosecond visible-NIR transient absorption spectroscopy (fsTAS) was used to investigate the excited-state dynamics of **Ir-PC**$^{5+}$ at shorter time scales (Figures 4, S28 and S29). When **Ir-PC**$^{5+}$ was investigated in neat acetonitrile, the excited-state decay upon 370 nm excitation was largely dominated by the ligand-centered state (^{3}LC, black spectrum in Figure 4 middle) but a small fraction, modeled as 20%, of a different excited state was also populated. We speculate this to be a charge-transfer-to-solvent state (^{3}CTSS, red spectrum in Figure 4 middle), as this novel state shows intense absorptions at 900 and 1050 nm and lacks the ^{3}LC characteristic transition at 560 nm. This ^{3}CTSS undergoes full charge separation in 40 ps, producing the corresponding $^3\{$**Ir-PC**$^{4+\bullet}$;$CH_3CN^{+\bullet}\}$ charge-separated state (^{3}CSS, blue spectrum in Figure 4 middle). Its differential spectrum features a NIR transition around 950 nm, a hallmark of the monoreduced **Ir-PC**$^{4+\bullet}$. ^{3}CSS decays in 2.4 ns, including charge recombination and perhaps irreversible photochemistry. When the experiments were carried out in the presence of 2 mM of trifluoroacetate, 370 nm excitation afforded a remarkably different scenario as the ^{3}CTSS was not observed. Instead, population of an excited state resembling the ^{3}LC, with a strong absorption at 560 nm, but with enhanced charge-transfer character manifested in enhanced NIR absorption above 800 nm was observed (^{3}LC, black spectrum in Figure 4 bottom). Its lifetime is drastically shortened from microseconds to 90 ps due to intraionic electron transfer to populate the corresponding ^{3}CSS, $^3\{$**Ir-PC**$^{4+\bullet}$;$CF_3COO^{\bullet}\}$ (^{3}CSS, blue

https://doi.org/10.1021/jacs.5c00129
J. Am. Chem. Soc. 2025, 147, 12082−12091

spectrum in Figure 4 bottom). This state showcases, next to a band at 990 nm from **Ir-PC**$^{4+\bullet}$, an additional signal peaking around 750 nm. This band should be interpreted with care, since it essentially overlaps with the fundamental wavelength of the laser system, but we hypothesize it might originate from an arene to $CF_3COO^\bullet$ charge transfer, similar to what is observed for arene to halogen charge transfer.[54−59] A large portion of this ^{3}CSS undergoes geminate charge recombination, in line with the small cage escape yields determined by nanosecond TAS.

We then turned to applying this novel ion-pairing approach to the trifluoromethylation of organic substrates. The optimization of trifluoromethylation factors (Table S1−S5), such as the equivalents of sodium trifluoroacetate and sodium persulfate ($Na_2S_2O_8$), yielded the reaction conditions presented in Table 1, i.e., an acetonitrile solution of 1,3,5-trimethoxybenzene, 10 mol % of **Ir-PC**$^{5+}$, 12.5 equiv of sodium trifluoroacetate and $Na_2S_2O_8$ as a terminal oxidant. The reaction was subject to 370 nm irradiation under argon which led to the formation of 2-trifluoromethyl-1,3,5-trimethoxybenzene with 60% yield, as determined by ^{19}F NMR spectroscopy using trifluoromethylbenzene as an internal standard. The reaction could be scaled up on a 4 mmol scale, which led to 360 mg (38% yield) of the desired isolated product. Control experiments in the absence of the photosensitizer, absence of the terminal oxidant or in the dark confirmed that these parameters are paramount for an efficient transformation. Interestingly, when the tricationic unmethylated $[Ir(tpy\text{-}Py)_2]^{3+}$ photosensitizer was used as control, the yield dropped from 60 to 26%. This decreased yield is tentatively attributed to a combination of a smaller binding constant (1.6 times smaller than **Ir-PC**$^{5+}$, Figure S11 and S12) as well as a smaller driving force for electron transfer (E_{red}* = 2.31 V vs 2.40 V vs NHE for **Ir-PC**$^{5+}$, Figure S13). Further evidence for the benefit of ion-pairing was gained from controlled experiments using 100 mM $TBAPF_6$, where the yield dropped to 32%. This decrease in yield originated from the charge screening effect that decreased the binding constant between CF_3COO^- and **Ir-PC**$^{5+}$. Additionally, when the photoredox transformation was carried out in DMSO or DMF, the trifluoromethylated product was undetectable. This immediately tracked with the inability to generate ion-pairs in these solvents, as demonstrated by titration experiments (Figure S14).

Table 1. Optimization of Arene Trifluoromethylation[a]

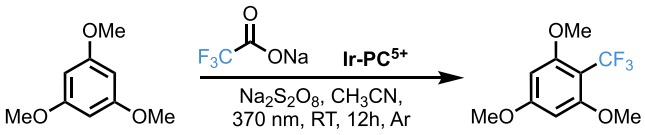

entry	deviation from standard conditions	yield/%
1	none	60
2	$[Ir(tpy\text{-}Py)_2]^{3+}$ instead of **Ir-PC**$^{5+}$	26
3	with 100 mM $TBAPF_6$	32
4	in DMSO	n.d.
5	in DMF	n.d.
6	without **Ir-PC**$^{5+}$	n.d.
7	without $Na_2S_2O_8$	<1
8	in the dark	n.d.
9	10% vol water	<1
10	4 mmol scale	38[b]

[a]Standard reaction conditions were as follows: arene (0.04 mmol, 1 equiv), CF_3COONa (12.5 equiv), **Ir-PC**$^{5+}$ (10 mol %), CH_3CN (2 mL), $Na_2S_2O_8$ (5 equiv), 12 h, room temperature (RT), 370 nm LED, Argon (Ar). n.d. = not detected. Yield for trifluoromethylated product was determined by ^{19}F NMR spectroscopy using trifluoromethylbenzene as an internal standard, unless otherwise specified. [b]Isolated yield.

The substrate scope was further investigated using **Ir-PC**$^{5+}$ and compared to other photosensitizers with similar or more positive driving forces for trifluoroacetate oxidation (Table 2). **Ir-PC**$^{5+}$ was capable of trifluoromethylating a wide range of substrates that included phenyl, pyridine, thiophene, pyrrole, and indole derivatives in yields that ranged from 30 to 60% (Table 2). The other photosensitizers, which included acridinium (Mes-Acr-Me$^+$$ClO_4^-$), triphenylpyridinium ($TPP^+$ BF_4^-), phenothiazine (PTH), and 2,3-dichloro-5,6-dicyano-1,4-benzoquinone (DDQ) were all inefficient at trifluoromethylating the investigated range of substrates. This negative result is actually paramount for the ion-pairing approach described herein. Indeed, based on excited-state reduction potentials, all the investigated photosensitizers are able to oxidize sodium trifluoroacetate, an aspect that was verified experimentally with the luminescent triphenylpyrilium (Figures S15 and S16) and acridinium (Figures S17 and S18) derivatives using Stern−Volmer experiments. However, none of these additional photosensitizers were able to form ion-pairs with trifluoroacetate (Figures S19−S22). Therefore, this excited-state reactivity solely relies on diffusion,[2] which is inefficient due to the short excited-state lifetime of these organic dyes. The lack of ion-pairing also implies that the oxidation of 1,3,5-trimethoxybenzene becomes competitive, as it is more easily oxidized by ∼0.85 V compared to trifluoroacetate. Furthermore, the ion-pairing process also influences the overall electrochemical response of the **Ir-PC**$^{5+}$-CF_3COO^- pair where a new electrochemical wave appeared at more negative potential than 2.3 V vs NHE (Figure S23). Thus, it appears that ion-pairing facilitates the trifluoroacetate oxidation, leading to the corresponding CO_2 and $CF_3^\bullet$ and preventing acetonitrile oxidation.

To further investigate the generality of this approach, we extended the scope to perfluoroacetate derivatives. As shown in Table 3, various perfluoroalkyl groups, including C_2F_5, C_3F_7, C_4F_9, C_5F_{11}, and C_6F_{13} groups, were successfully incorporated onto the 1,3,5-trimethoxybenzene backbone. Taken altogether, the yields evolve from 60% for the trifluoromethylation reaction, to 17% for C_6F_{13}, in line with the radical polarity of the respective reactive radicals.[60] Motivated by the broad substrate scope that could be selectively functionalized, we transposed our approach to the trifluoromethylation of natural products and pharmaceutical molecules (Table 4). The reaction was overall successful, achieving the desired transformation with 20−24% isolated yields after preparative HPLC purification.

Taken altogether, the experimental data confirmed that the overall ion-paired-mediated perfluoroalkylation is broadly applicable. We were however interested in gaining more information about the benefits of this ion-paired approach as well as to confirm that the reaction proceeds via the formation of CF_3 radicals. For that, a photoreaction was carried out in the presence of TEMPO that was used as radical trapping agent. The formation of the TEMPO−CF_3 adduct was clearly identified by ^{19}F NMR spectroscopy and GC-MS analysis (Figures S24 and S25).

https://doi.org/10.1021/jacs.5c00129
J. Am. Chem. Soc. 2025, 147, 12082−12091

Table 2. Substrate Scope of Trifluoromethylation[a]

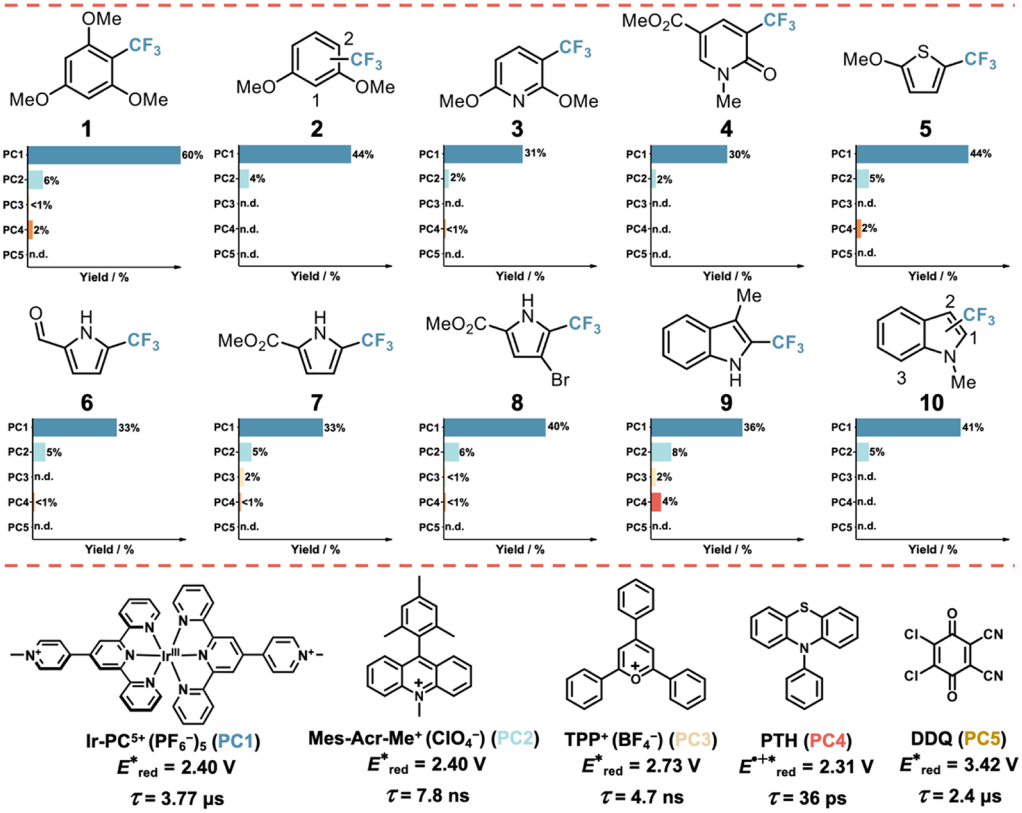

[a]Reaction conditions were as follows: arene (0.04 mmol, 1 equiv), CF_3COONa (12.5 equiv), PC (10 mol %), CH_3CN (2 mL), $Na_2S_2O_8$ (5 equiv), 12 h, room temperature (RT), 370 nm LED, argon. n.d. = not detected. Yield for trifluoromethylated product was determined by ^{19}F NMR spectroscopy using trifluoromethylbenzene as an internal standard. Note that the excited-state reduction potential of $PTH^{\bullet+}$ is reported as we expect this species to be formed in solution and to be the only one competent for trifluoroacetate oxidation.

Table 3. Scope of Perfluoroalkyl Carboxylates for the Perfluoroalkylation[a]

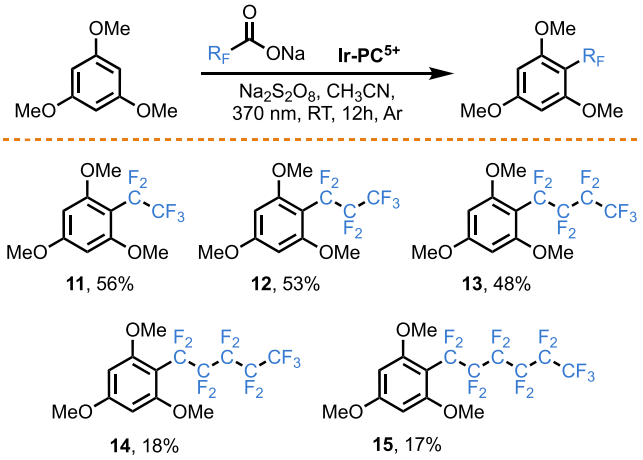

[a]Standard reaction conditions were as follows: arene (0.04 mmol, 1 equiv), perfluoroalkyl carboxylates (12.5 equiv), PC (10 mol %), CH_3CN (2 mL), $Na_2S_2O_8$ (5 equiv), 12 h, room temperature (RT), 370 nm LED, Argon. Yields for perfluoroalkylation product were determined by ^1H NMR spectroscopy using pyrazine as an internal standard.

Table 4. Trifluoromethylation of Natural Products and Pharmaceuticals[a]

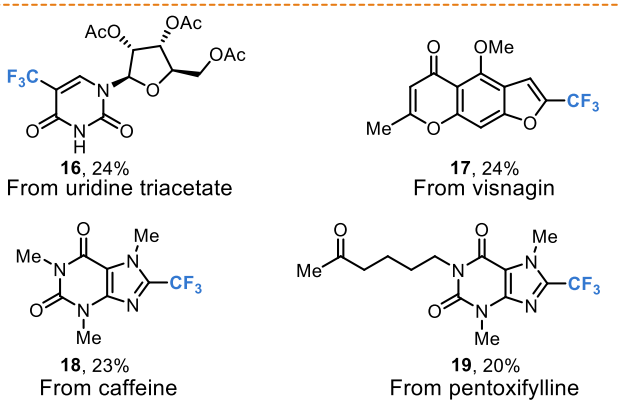

[a]Standard reaction conditions were as follows: substrate (0.1 mmol, 1 equiv), CF_3COONa (12.5 equiv), **Ir-PC**$^{5+}$ (10 mol %), CH_3CN (2 mL), $Na_2S_2O_8$ (5 equiv), 20 h, room temperature (RT), 370 nm LED, Argon. The products were purified by prep-HPLC.

The benefits of ion-pairing were clearly visible when Stern–Volmer experiments were carried out in the presence of the S1–S10 substrates (structures showed in Table 2). Based on electrochemistry measurements (Figure S26), these substrates are all competent for reductive excited-state electron transfer with driving forces (ΔG_{et}) that range from −0.45 eV for substrate S4 to −1.29 eV for substrate S9. The driving force for the oxidation of trifluoroacetate is only ∼ −0.10 eV.

https://doi.org/10.1021/jacs.5c00129
J. Am. Chem. Soc. 2025, 147, 12082−12091

Quenching rate constants ranged from 1.3×10^{10} M^{-1} s^{-1} for substrate S9 to 5.8×10^{9} M^{-1} s^{-1} for substrate S4, in line with thermodynamic expectations (Table 5). The large quenching rate constant ($k_q = 1.5 \times 10^{11}$ M^{-1} s^{-1}) for trifluoroacetate stands in contrast to thermodynamic considerations. In addition, ion-pairing promotes the preassociation of the reactive species which favors trifluoroacetate oxidation over all other substrates.

Table 5. Driving Force (ΔG) for Excited-state Electron Transfer from the Substrate (Structure Indicated in Table 2) to the Excited Ir-PC^{5+} as Well as the Corresponding Quenching Rate Constant Determined by Stern−Volmer Quenching Experiments (Figure S27)

substrate	ΔG (eV)	k_q (10^9 M^{-1} s^{-1})
S1	−0.94	8.0
S2	−0.77	7.8
S3	−0.69	6.6
S4	−0.45	5.8
S5	−0.92	10
S6	−0.53	6.3
S7	−0.58	5.8
S8	−0.55	5.7
S9	−1.29	13
S10	−1.22	13
CF_3COONa	−0.09	150[a]

[a]In addition to this large quenching rate constant afforded by the Coulombic attraction between **Ir-PC^{5+}** and trifluoroacetate, a static quenching constant (K_S) of 5.3×10^4 M^{-1} was also observed (Figure 3).

Taken altogether, the data gathered herein allows to propose a reaction mechanism depicted in Figure 5. Ion-pair between **Ir-PC^{5+}** and trifluoroacetate takes place in the ground state in acetonitrile. Light excitation populates an excited state that undergoes intra-ion-pair electron transfer, as indicated by femtosecond UV−visible transient absorption spectroscopy as well as by the static quenching observed in Stern−Volmer experiments. This generates the reduced **Ir-PC$^{4+\bullet}$** and the corresponding $CF_3COO^{\bullet}$ with a cage escape yield of 0.056. **Ir-PC^{5+}** is regenerated through the use of the $Na_2S_2O_8$ external oxidant whereas the $CF_3COO^{\bullet}$ radical undergoes homolytic bond cleavage to generate CO_2 and the corresponding $CF_3^{\bullet}$, as verified by radical trapping experiments (Figures S24 and S25). This radical is then able to react with the aromatic ring, which, following proton loss and oxidative rearomatization, yields the final desired product.

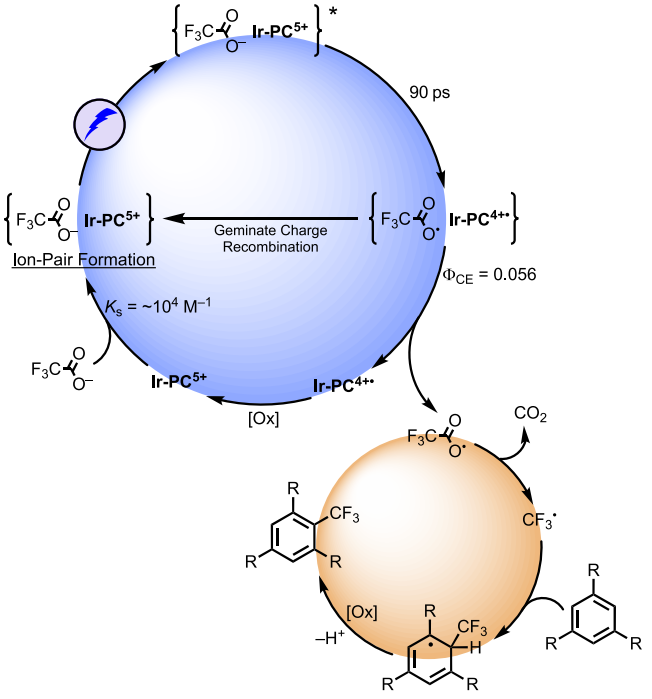

Figure 5. Proposed reaction mechanism operating via the ion-pair formation between **Ir-PC^{5+}** and trifluoroacetate.

CONCLUSIONS

Ion-pair formation between trifluoroacetate and a pentacationic Ir(III) photosensitizer resulted in the formation of $CF_3^{\bullet}$ and the reduced photosensitizer. The $CF_3^{\bullet}$ photoproduct was shown to trifluoromethylate a wide range of substrates that included phenyl, pyridine, thiophene, pyrrole, and indole derivatives in yields that range from 30 to 60%. The reaction was also exemplified on natural and pharmaceutically relevant substrates. The moderate yields probably originate from small cage escape yields (0.056). The generality of this reaction was further exemplified through the introduction of various perfluoroalkyl groups, including C_2F_5, C_3F_7, C_4F_9, C_5F_{11}, and C_6F_{13} groups. This implies that this approach could also be used for the removal and/or use of perfluoroalkyl substances (PFAS). Importantly, control experiments with photosensitizers that were able to oxidize trifluoroacetate but unable to form strong ion-pairs did not efficiently drive the trifluoromethylation reaction. Thus, this ion-pair photoredox catalysis strategy not only allows one to circumvent solvent and substrate oxidation for trifluoromethylation but also impacts the product yield. Hence, our new concept presented herein is an important contribution on the way to an extended use of sodium trifluoroacetate as $CF_3^{\bullet}$ source and could be applicable to other very potent photooxidants.[59,61] Such a concept is highly relevant for future developments as CF_3COONa is abundant, cheap and atom economic as the only side product generated through that oxidation is CO_2.

ASSOCIATED CONTENT

Supporting Information

The Supporting Information is available free of charge at https://pubs.acs.org/doi/10.1021/jacs.5c00129.

Experimental section, additional spectroscopic characterizations, additional reaction optimizations (PDF)

AUTHOR INFORMATION

Corresponding Authors

Ke Hu − *School of Chemical Science and Engineering, Tongji University, Shanghai 200092, P. R. China; Department of Chemistry and Shanghai Key Laboratory of Molecular Catalysis and Innovative Materials, Fudan University, Shanghai 200433, P. R. China;* orcid.org/0000-0002-0240-7192; Email: khu@tongji.edu.cn

Ludovic Troian-Gautier − *UCLouvain, Institute of Condensed Matter and Nanosciences (IMCN), Molecular Chemistry, Materials and Catalysis (MOST), 1348 Louvain-la-Neuve, Belgium; Wel Research Institute, 1300 Wavre,*

https://doi.org/10.1021/jacs.5c00129
J. Am. Chem. Soc. 2025, 147, 12082−12091

Belgium; orcid.org/0000-0002-7690-1361; Email: Ludovic.Troian@uclouvain.be

Authors

Pengju Li − *Department of Chemistry and Shanghai Key Laboratory of Molecular Catalysis and Innovative Materials, Fudan University, Shanghai 200433, P. R. China*

Céline Bourgois − *UCLouvain, Institute of Condensed Matter and Nanosciences (IMCN), Molecular Chemistry, Materials and Catalysis (MOST), 1348 Louvain-la-Neuve, Belgium;* orcid.org/0009-0006-1080-6560

Felix Glaser − *UCLouvain, Institute of Condensed Matter and Nanosciences (IMCN), Molecular Chemistry, Materials and Catalysis (MOST), 1348 Louvain-la-Neuve, Belgium;* orcid.org/0000-0002-6717-916X

Simon De Kreijger − *UCLouvain, Institute of Condensed Matter and Nanosciences (IMCN), Molecular Chemistry, Materials and Catalysis (MOST), 1348 Louvain-la-Neuve, Belgium*

Alejandro Cadranel − *Departamento de Química Inorgánica, Analítica y Química Física, Universidad de Buenos Aires, Facultad de Ciencias Exactas y Naturales, C1428EHA Buenos Aires, Argentina; CONICET − Universidad de Buenos Aires, Instituto de Química-Física de Materiales, Medio Ambiente y Energía (INQUIMAE), C1428EHA Buenos Aires, Argentina; Physical Chemistry I and Interdisciplinary Center for Molecular Materials, Friedrich-Alexander-Universität Erlangen-Nürnberg (FAU), 91058 Erlangen, Germany;* orcid.org/0000-0002-6597-4397

Complete contact information is available at: https://pubs.acs.org/10.1021/jacs.5c00129

Author Contributions

All authors have given approval to the final version of the manuscript.

Notes

The authors declare no competing financial interest.

■ ACKNOWLEDGMENTS

P.L. and K.H. acknowledge the financial support from the National Key R&D Program of China (2023YFE0124100) and the National Natural Science Foundation of China (22173022, 22311530694). This work was also supported by the Fonds de la Recherche Scientifique (F.R.S.-FNRS) through the PINT-Bilat-M n° R.M013.23 funding scheme. This work was further supported by the "Action de Recherche Concertée" through the project "UNCAGED" under grant no. 23/28-135. L.T.-G. is a Chercheur Qualifié of the Fonds de la Recherche Scientifique − FNRS. F.G. is a chargé de recherches of the Fonds de la Recherche Scientifique − FNRS. C.B., F.G., S.D.K. and L.T.-G. gratefully acknowledge the UCLouvain for financial support. A.C. is a member of the research staff of CONICET.

■ REFERENCES

(1) Glaser, F.; Kerzig, C.; Wenger, O. S. Multi-Photon Excitation in Photoredox Catalysis: Concepts, Applications Methods. *Angew. Chem. Int. Ed.* **2020**, *59*, 10266−10284.

(2) De Kreijger, S.; Glaser, F.; Troian-Gautier, L. From Photons to Reactions: Key Concepts in Photoredox Catalysis. *Chem. Catal.* **2024**, *4*, No. 101110.

(3) Hoffmann, N. Combining Photoredox and Metal Catalysis. *ChemCatChem* **2015**, *7*, 393−394.

(4) Chan, A. Y.; Perry, I. B.; Bissonnette, N. B.; Buksh, B. F.; Edwards, G. A.; Frye, L. I.; Garry, O. L.; Lavagnino, M. N.; Li, B. X.; Liang, Y.; et al. Metallaphotoredox: The Merger of Photoredox and Transition Metal Catalysis. *Chem. Rev.* **2022**, *122*, 1485−1542.

(5) Romero, N. A.; Nicewicz, D. A. Organic Photoredox Catalysis. *Chem. Rev.* **2016**, *116*, 10075−10166.

(6) Tay, N. E. S.; Lehnherr, D.; Rovis, T. Photons or Electrons? A Critical Comparison of Electrochemistry and Photoredox Catalysis for Organic Synthesis. *Chem. Rev.* **2022**, *122*, 2487−2649.

(7) Glaser, F.; Wenger, O. S. Recent Progress in the Development of Transition-Metal Based Photoredox Catalysts. *Coord. Chem. Rev.* **2020**, *405*, No. 213129.

(8) Shaw, M. H.; Twilton, J.; MacMillan, D. W. C. Photoredox Catalysis in Organic Chemistry. *J. Org. Chem.* **2016**, *81*, 6898−6926.

(9) Ilardi, E. A.; Vitaku, E.; Njardarson, J. T. Data-Mining for Sulfur and Fluorine: An Evaluation of Pharmaceuticals to Reveal Opportunities for Drug Design and Discovery. *J. Med. Chem.* **2014**, *57*, 2832−2842.

(10) Inoue, M.; Sumii, Y.; Shibata, N. Contribution of Organofluorine Compounds to Pharmaceuticals. *ACS Omega* **2020**, *5*, 10633−10640.

(11) Han, J.; Kiss, L.; Mei, H.; Remete, A. M.; Ponikvar-Svet, M.; Sedgwick, D. M.; Roman, R.; Fustero, S.; Moriwaki, H.; Soloshonok, V. A. Chemical Aspects of Human and Environmental Overload with Fluorine. *Chem. Rev.* **2021**, *121*, 4678−4742.

(12) Mizuta, S.; Galicia-López, O.; Engle, K. M.; Verhoog, S.; Wheelhouse, K.; Rassias, G.; Gouverneur, V. Trifluoromethylation of Allylsilanes under Copper Catalysis. *Chem. - Eur. J.* **2012**, *18*, 8583−8587.

(13) Barata-Vallejo, S.; Lantaño, B.; Postigo, A. Recent Advances in Trifluoromethylation Reactions with Electrophilic Trifluoromethylating Reagents. *Chem. - Eur. J.* **2014**, *20*, 16806−16829.

(14) Charpentier, J.; Früh, N.; Togni, A. Electrophilic Trifluoromethylation by Use of Hypervalent Iodine Reagents. *Chem. Rev.* **2015**, *115*, 650−682.

(15) Wang, S.-M.; Han, J.-B.; Zhang, C.-P.; Qin, H.-L.; Xiao, J.-C. An Overview of Reductive Trifluoromethylation Reactions Using Electrophilic '+Cf3' Reagents. *Tetrahedron* **2015**, *71*, 7949−7976.

(16) Langlois, B. R.; Billard, T.; Roussel, S. Nucleophilic Trifluoromethylation: Some Recent Reagents and Their Stereoselective Aspects. *J. Fluorine Chem.* **2005**, *126*, 173−179.

(17) Tomashenko, O. A.; Grushin, V. V. Aromatic Trifluoromethylation with Metal Complexes. *Chem. Rev.* **2011**, *111*, 4475−4521.

(18) Eisenberger, P.; Gischig, S.; Togni, A. Novel 10-I-3 Hypervalent Iodine-Based Compounds for Electrophilic Trifluoromethylation. *Chem. - Eur. J.* **2006**, *12*, 2579−2586.

(19) Teruo, U.; Sumi, I. Power-Variable Trifluoromethylating Agents, (Trifluoromethyl)Dibenzothio- and -Selenophenium Salt System. *Tetrahedron Lett.* **1990**, *31*, 3579−3582.

(20) Umemoto, T.; Ishihara, S. Power-Variable Electrophilic Trifluoromethylating Agents. S-, Se-, and Te-(Trifluoromethyl)-Dibenzothio-, -Seleno-, and -Tellurophenium Salt System. *J. Am. Chem. Soc.* **1993**, *115*, 2156−2164.

(21) Yang, J.-J.; Kirchmeier, R. L. Shreeve, J. n. M., New Electrophilic Trifluoromethylating Agents. *J. Org. Chem.* **1998**, *63*, 2656−2660.

(22) Matsnev, A.; Noritake, S.; Nomura, Y.; Tokunaga, E.; Nakamura, S.; Shibata, N. Efficient Access to Extended Yagupolskii−Umemoto-Type Reagents: Triflic Acid Catalyzed Intramolecular Cyclization of Ortho-Ethynylaryltrifluoromethylsulfanes. *Angew. Chem., Int. Ed.* **2010**, *49*, 572−576.

(23) Beatty, J. W.; Douglas, J. J.; Cole, K. P.; Stephenson, C. R. J. A Scalable and Operationally Simple Radical Trifluoromethylation. *Nat. Commun.* **2015**, *6*, No. 7919.

(24) Lai, C.; Mallouk, T. E.; New, A. Approach to the Photochemical Trifluoromethylation of Aromatic Compounds. *J. Chem. Soc. Chem. Comm.* **1993**, 1359−1361.

(25) Bian, K.-J.; Lu, Y.-C.; Nemoto, D.; Kao, S.-C.; Chen, X.; West, J. G. Photocatalytic Hydrofluoroalkylation of Alkenes with Carboxylic Acids. *Nat. Chem.* **2023**, *15*, 1683−1692.
(26) Chen, Y.; He, Y.; Gao, Y.; Xue, J.; Qu, W.; Xuan, J.; Mo, Y. Scalable Decarboxylative Trifluoromethylation by Ion-Shielding Heterogeneous Photoelectrocatalysis. *Science* **2024**, *384*, 670−676.
(27) Qi, J.; Xu, J.; Ang, H. T.; Wang, B.; Gupta, N. K.; Dubbaka, S. R.; O'Neill, P.; Mao, X.; Lum, Y.; Wu, J. Electrophotochemical Synthesis Facilitated Trifluoromethylation of Arenes Using Trifluoroacetic Acid. *J. Am. Chem. Soc.* **2023**, *145*, 24965−24971.
(28) Yin, D.; Su, D.; Jin, J. Photoredox Catalytic Trifluoromethylation and Perfluoroalkylation of Arenes Using Trifluoroacetic and Related Carboxylic Acids. *Cell. Rep. Phys. Sci.* **2020**, *1*, No. 100141, DOI: 10.1016/j.xcrp.2020.100141.
(29) Zhang, M.; Chen, J.; Huang, S.; Xu, B.; Lin, J.; Su, W. Photocatalytic Fluoroalkylations of (Hetero)Arenes Enabled by the Acid-Triggered Reactivity Umpolung of Acetoxime Esters. *Chem. Catal.* **2022**, *2*, 1793−1806.
(30) Campbell, B. M.; Gordon, J. B.; Raguram, E. R.; Gonzalez, M. I.; Reynolds, K. G.; Nava, M.; Nocera, D. G. Electrophotocatalytic Perfluoroalkylation by LMCT Excitation of Ag(II) Perfluoroalkyl Carboxylates. *Science* **2024**, *383*, 279−284.
(31) Herbstritt, D.; Braun, T. Reduction of SF5CF3 via Iridium Catalysis: Radical Trifluoromethylation of Aromatics. *Chem. Commun.* **2023**, *59*, 3850−3853.
(32) Egami, H.; Ito, Y.; Ide, T.; Masuda, S.; Hamashima, Y. Simple Photo-Induced Trifluoromethylation of Aromatic Rings. *Synthesis* **2018**, *50*, 2948−2953.
(33) Lin, J.; Li, Z.; Kan, J.; Huang, S.; Su, W.; Li, Y. Photo-Driven Redox-Neutral Decarboxylative Carbon-Hydrogen Trifluoromethylation of (Hetero)Arenes with Trifluoroacetic Acid. *Nat. Commun.* **2017**, *8*, No. 14353.
(34) Bazyar, Z.; Hosseini-Sarvari, M. Au@Zno Core−Shell: Scalable Photocatalytic Trifluoromethylation Using CF3CO2Na as an Inexpensive Reagent under Visible Light Irradiation. *Org. Process Res. Dev.* **2019**, *23*, 2345−2353.
(35) Fernández-García, S.; Chantzakou, V. O.; Juliá-Hernández, F. Direct Decarboxylation of Trifluoroacetates Enabled by Iron Photocatalysis. *Angew. Chem., Int. Ed.* **2024**, *63*, No. e202311984.
(36) Jiang, X.; Lan, Y.; Hao, Y.; Jiang, K.; He, J.; Zhu, J.; Jia, S.; Song, J.; Li, S.-J.; Niu, L. Iron Photocatalysis Via Brønsted Acid-Unlocked Ligand-to-Metal Charge Transfer. *Nat. Commun.* **2024**, *15*, No. 6115.
(37) Juliá, F. Ligand-to-Metal Charge Transfer (Lmct) Photochemistry at 3d-Metal Complexes: An Emerging Tool for Sustainable Organic Synthesis. *ChemCatChem* **2022**, *14*, No. e202200916.
(38) Glaser, F.; Aydogan, A.; Elias, B.; Troian-Gautier, L. The Great Strides of Iron Photosensitizers for Contemporary Organic Photoredox Catalysis: On Our Way to the Holy Grail? *Coord. Chem. Rev.* **2024**, *500*, No. 215522.
(39) Huang, Q.; Lou, C.; Lv, L.; Li, Z. Photoinduced Fluoroalkylation-Peroxidation of Alkenes Enabled by Ligand-to-Iron Charge Transfer Mediated Decarboxylation. *Chem. Commun.* **2024**, *60*, 12389−12392.
(40) Zhang, K.; Rombach, D.; Nötel, N. Y.; Jeschke, G.; Katayev, D. Radical Trifluoroacetylation of Alkenes Triggered by a Visible-Light-Promoted C−O Bond Fragmentation of Trifluoroacetic Anhydride. *Angew. Chem., Int. Ed.* **2021**, *60*, 22487−22495.
(41) Vander Wee-Léonard, M.; Elias, B.; Troian-Gautier, L. Photoinduced One-Electron Chloride Oxidation in Water Using a Pentacationic Ir(III) Photosensitizer. *J. Am. Chem. Soc.* **2024**, *146*, 11031−11035.
(42) Glaser, F.; Schmitz, M.; Kerzig, C. Coulomb Interactions for Mediator-Enhanced Sensitized Triplet−Triplet Annihilation Upconversion in Solution. *Nanoscale* **2023**, *16*, 123−137.
(43) Schmitz, M.; Bertrams, M.-S.; Sell, A. C.; Glaser, F.; Kerzig, C. Efficient Energy and Electron Transfer Photocatalysis with a Coulombic Dyad. *J. Am. Chem. Soc.* **2024**, *146*, 25799−25812.
(44) Benesi, H. A.; Hildebrand, J. H. A Spectrophotometric Investigation of the Interaction of Iodine with Aromatic Hydrocarbons. *J. Am. Chem. Soc.* **1949**, *71*, 2703−2707.
(45) Ward, W. M.; Farnum, B. H.; Siegler, M.; Meyer, G. J. Chloride Ion-Pairing with Ru(II) Polypyridyl Compounds in Dichloromethane. *J. Phys. Chem. A* **2013**, *117*, 8883−8894.
(46) Murov, S. L.; Carmichael, I.; Hug, G. L. *Handbook of Photochemistry*, 2nd ed.; Marcel Dekker, Inc: New York, 1993.
(47) Wehlin, S. A. M.; Troian-Gautier, L.; Sampaio, R. N.; Marcélis, L.; Meyer, G. J. Ter-Ionic Complex That Forms a Bond Upon Visible Light Absorption. *J. Am. Chem. Soc.* **2018**, *140*, 7799−7802.
(48) Wehlin, S. A. M.; Troian-Gautier, L.; Li, G.; Meyer, G. J. Chloride Oxidation by Ruthenium Excited-States in Solution. *J. Am. Chem. Soc.* **2017**, *139*, 12903−12906.
(49) Elliot, A. J.; McCracken, D. R.; Buxton, G. V.; Wood, N. D. Estimation of Rate Constants for near-Diffusion-Controlled Reactions in Water at High Temperatures. *J. Chem. Soc., Faraday Trans.* **1990**, *86*, 1539−1547.
(50) Swords, W. B.; Li, G.; Meyer, G. J. Iodide Ion Pairing with Highly Charged Ruthenium Polypyridyl Cations in Ch3cn. *Inorg. Chem.* **2015**, *54*, 4512−4519.
(51) Troian-Gautier, L.; Swords, W. B.; Meyer, G. J. Iodide Photoredox and Bond Formation Chemistry. *Acc. Chem. Res.* **2019**, *52*, 170−179.
(52) Goodwin, M. J.; Dickenson, J. C.; Ripak, A.; Deetz, A. M.; McCarthy, J. S.; Meyer, G. J.; Troian-Gautier, L. Factors That Impact Photochemical Cage Escape Yields. *Chem. Rev.* **2024**, *124*, 7379−7464.
(53) Ripak, A.; De Kreijger, S.; Sampaio, R. N.; Vincent, C. A.; Cauët, É.; Jabin, I.; Tambar, U. K.; Elias, B.; Troian-Gautier, L. Photosensitized Activation of Diazonium Derivatives for C−B Bond Formation. *Chem. Catal.* **2023**, *3*, No. 100490.
(54) Förgeteg, S.; Bérces, T. Laser Flash Photolysis Study of Chlorine Atom/Simple Arene π-Complexes in Carbon Tetrachloride and Acetonitrile. *J. Photochem. Photobiol., A* **1993**, *73*, 187−195.
(55) Bühler, R. E.; Ebert, M. Transient Charge-Transfer Complexes with Chlorine Atoms by Pulse Radiolysis of Carbon Tetrachloride Solutions. *Nature* **1967**, *214*, 1220−1221.
(56) Bossy, J. M.; Buehler, R. E.; Ebert, M. Pulse Radiolysis of Organic Halogen Compounds. II. Transient Bromine-Atom Charge-Transfer Complexes Observed by Pulse Radiolysis. *J. Am. Chem. Soc.* **1970**, *92*, 1099−1101.
(57) Strong, R. L.; Rand, S. J.; Britt, J. A. Charge-Transfer Spectra of Iodine Atom-Aromatic Hydrocarbon Complexes1. *J. Am. Chem. Soc.* **1960**, *82*, 5053−5057.
(58) Hwang, S. J.; Anderson, B. L.; Powers, D. C.; Maher, A. G.; Hadt, R. G.; Nocera, D. G. Halogen Photoelimination from Monomeric Nickel(III) Complexes Enabled by the Secondary Coordination Sphere. *Organometallics* **2015**, *34*, 4766−4774.
(59) De Kreijger, S.; Elias, B.; Troian-Gautier, L. Chloride, Bromide, and Iodide Photooxidation in Acetonitrile/Water Mixtures Using Binuclear Iridium(III) Photosensitizers. *Inorg. Chem.* **2023**, *62*, 16196−16202.
(60) Garwood, J. J. A.; Chen, A. D.; Nagib, D. A. Radical Polarity. *J. Am. Chem. Soc.* **2024**, *146*, 28034−28059.
(61) East, N. R.; Naumann, R.; Förster, C.; Ramanan, C.; Diezemann, G.; Heinze, K. Oxidative Two-State Photoreactivity of a Manganese(Iv) Complex Using near-Infrared Light. *Nat. Chem.* **2024**, *16*, 827−834.